Journal of Biomechanics 45 (2012) 1959–1964

Contents lists available at SciVerse ScienceDirect

Journal of Biomechanics

journal homepage: www.elsevier.com/locate/jbiomech
www.JBiomech.com

Fracture risk in the femoral hip region: A finite element analysis supported experimental approach

Alexander Tsouknidas [a,*], Kleovoulos Anagnostidis [b], Georgios Maliaris [c], Nikolaos Michailidis [d]

[a] Laboratory for Machine Tools and Manufacturing Engineering, Mechanical Engineering Department, Aristoteles University of Thessaloniki, 54124 Thessaloniki, Greece
[b] 3rd Orthopaedic Department "Papageorgiou" General Hospital, Aristoteles University of Thessaloniki, Greece
[c] Department of Electrical and Computer Engineering, Democritus University of Thrace, Xanthi, Greece
[d] Physical Metallurgy Laboratory, Mechanical Engineering Department, Aristoteles University of Thessaloniki, Greece

ARTICLE INFO

Article history:
Accepted 9 May 2012

Keywords:
Femoral hip
FEA
Dual-energy X-ray absorptiometry
Fracture risk indicator

ABSTRACT

The decrease of bone mineral density (BMD) is a multifactorial bone pathology, commonly referred to as osteoporosis. The subsequent decline of the bone's micro-structural characteristics renders the human skeletal system, and especially the hip, susceptible to fragility fractures. This study represents a systematic attempt to correlate BMD spectrums to the mechanical strength characteristics of the femoral neck and determine a fracture risk indicator based on non-invasive imaging techniques. The BMD of 30 patients' femurs was measured in vivo by Dual-energy X-ray absorptiometry (DXA). As these patients were subjected to total hip replacement, the mechanical strength properties of their femurs' were determined ex-vivo using uniaxial compression experiments. FEA simulations facilitated the correlation of the DXA measurements to the apparent fracture risk, indicating critical strain values during complex loading scenarios.

1. Introduction

Osteoporosis is a multifactorial bone disease concerning roughly 4% of the human population (Melton et al., 1992). As an asymptomatic condition, osteoporosis fails to exhibit noticeable symptoms, particularly at early stages and thus is usually under-diagnosed. Untreated however, this clinically silent disease is likely to increase the risk of fragility fractures (Ettinger, 2008; Rockwood et al., 1990; Cooper et al., 1992). Due to its high morbidity and global nature, osteoporosis is considered a pathology with a significant socioeconomic impact (Ray et al., 1997).

The affected patients' bone mineral density (BMD) is drastically reduced, deteriorating the bones' micostructural characteristics as a result of excessive bone resorption followed by insufficient bone formation during remodelling (Frost and Thomas, 1963; Raisz, 2005). The pathogenesis has been associated to dietary aspects (Hackett et al., 2009), immobilisation (Minaire, 1989), hyper-parathyroidism (Dupree and Dobs, 2004), vitamin D deficiency (Holick, 2004), alteration of biochemical markers like hormones (Parfitt et al., 1995; Black et al., 2003) and aging (Newton-John and Morgan, 1970). Regardless of aetiology, decreased bone mineral density renders the skeletal system susceptible to fracture, predominantly occurring at the hip (Bohr and Schaadt, 1985), the vertebral column (Old and Calvert, 2004) and wrist (Dempster, 2011).

According to the World Health Organisation, osteopenia and osteoporosis are defined by the patient's bone mass deviation, when compared to that of an average, young and healthy adult (World Health Organisation, 1994) when measured by DXA.

Even though DXA can accurately determine the minerals and lean soft tissue of the examined area, the overall accuracy of the measurement is impaired by the subtraction of the indirectly calculated fat mass (St-Onge et al., 2004). Furthermore, DXA results are represented as mass per area, thus not considering the anisotropy of the bone tissue and are hence a qualitative and not quantitative index of the bone structure (Lochmuller et al., 2000).

Several other methods have been recently introduced to determine bone mineral density (Genant et al., 1996; Braun et al., 1998); DXA nevertheless is still widely considered as the method of choice. Other techniques like peripheral quantitative computed tomography (pQCT) may be accurate in measuring BMD at peripheral skeletal sites; however they exhibit restrictions that prohibit measurements at the proximal femur (Augat et al., 1996, 1998).

The aim of this investigation is to determine the correlation of the bone mineral density in the femoral neck, as measured by DXA, to experimentally determined strength characteristics of the bone. This, followed by the introduced FEA simulation, will facilitate the use of DXA as an indicator of fragility fracture risk

* Corresponding author. Tel.: +30 2310 995940; fax: +30 2310 996059.
E-mail address: alextso@auth.gr (A. Tsouknidas).

0021-9290/$ - see front matter © 2012 Elsevier Ltd. All rights reserved.
http://dx.doi.org/10.1016/j.jbiomech.2012.05.011

in the hip region, as there is a consensus throughout literature that hip fractures involve the most severe consequences of osteoporotic bone loss.

2. Materials and methods

This study was conducted on femoral neck samples, harvested from patients undergoing total hip replacement due to osteoarthritis. Written consent was obtained in all cases. In order to determine the samples' structural integrity, standard X-rays (anterior–posterior) of the pelvis were taken preoperatively in all cases. Patients with a short femoral neck, large cysts in neck region or previous surgeries in proximal femur were excluded from the study.

Overall 30 patients (27 female and 3 male) were considered as representative candidates for this study and thus subjected to DXA, to catalogue their proximal femur bone mineral density. The average age of these patients was 63.7 years (57–76 years).

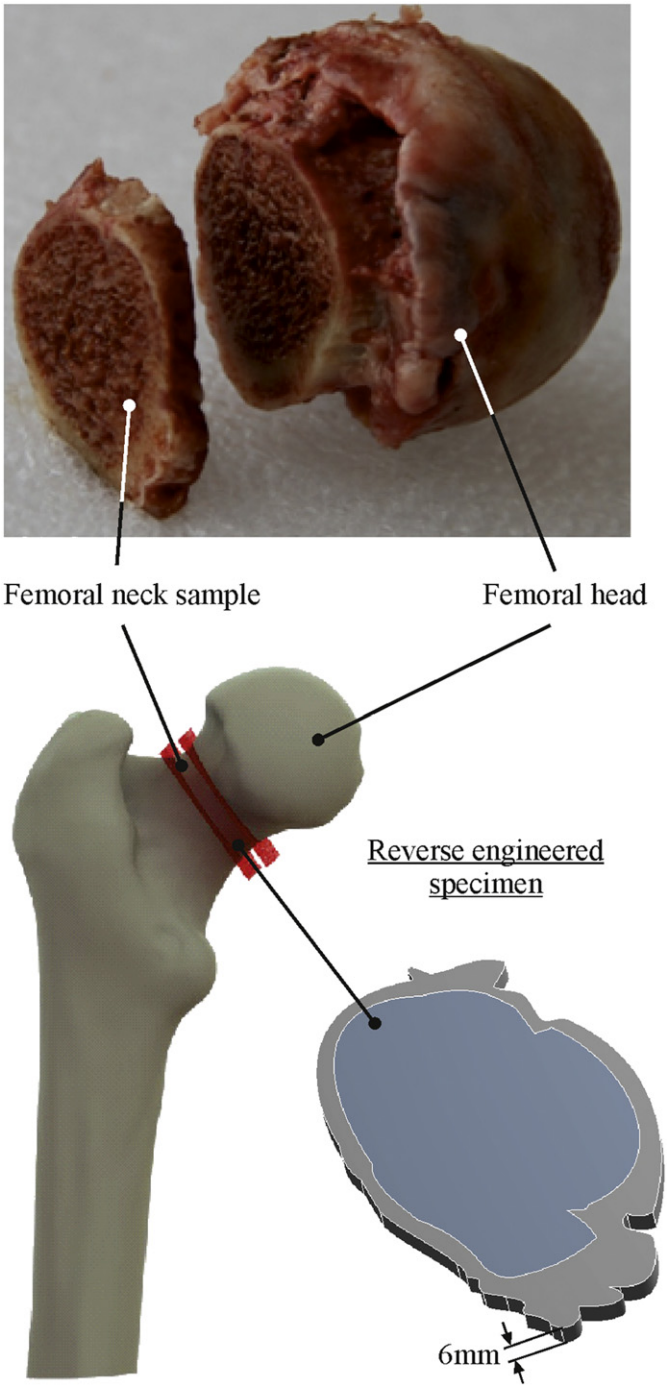

Fig. 1. Considered bone specimen and reverse engineered model.

During the surgical procedure and after a 45° osteotomy, femoral heads were removed and stored at −60 °C until evaluation. A plane bone slice with 6 mm thickness was harvested from the femoral neck (see Fig. 1) as two parallel blades, mounted on a mechanical saw at a 6 mm distance, simultaneously entered the proximal femur (as signified by the two parallel read planes of Fig. 1). This ensured similarity among all specimens while producing parallel piped specimens, directly employable in compression tests.

Mechanical testing was performed on an electric INSTRON Testing system. To determine the specimens' strength characteristics, all samples were subjected to uniaxial compression, until failure. A cross-head travelling speed of 0.6 mm/s was selected and the maximum travelling distance (upon contact) was set to 5 mm in order to avoid contact of the moving cross-head and the fixed base plate. To reduce friction, the sample–actuator contact areas were lubricated. The displacement of the cross-head was measured by means of an inductive sensor, at an accuracy of 1 μm.

Prior to the destructive testing, all specimens were photographed perpendicular to both their sides and an image analysis software allowed the determination of the examined surface's area. This parameter was used further on during the calculation of the specimens' biomechanical parameters (elasticity modulus and yield stress), which were correlated to the BMD using the Pearson correlation coefficient (r) and a linear regression model.

30 experiments were conducted to determine both compressive yield strength and modulus of elasticity and associate these to the DXA measurements. DXA determines bone mineral density in terms of T-score, which is a relative indicator of bone quality, comparing the measured BMD to that of a young adult (at the age of 35) of the same gender with peak bone mass. In these terms both male and female samples can be considered concertedly, as T-score represents a gender free statistical value.

3. Results

A correlation of characteristic and mean values (BMD and T-score) determined by DXA measurements to the corresponding mechanical properties (yield stress and elastic modulus) of the examined specimens is reflected in Table 1. The Young modulus values (E) are in good coherence with previously presented data covering similar spectrums 12.643–28.536 GPa (in our study), 10.4–19.3 GPa (Keller et al., 1990) and a mean value of 18.2 GPa according to Reilly and Burstein (1997). The determined yield stress values 109.448–218.02 MPa also converged to previous studies 115–209 MPa (Keller et al., 1990) and the mean value of 114 Mpa determined earlier by Reilly and Burstein (1997).

The offset in the determined values can be attributed to the different sampling sites and techniques of the compared studies.

A significant dependency of the femoral neck's yield stress and elastic modulus to the measured T-score was affirmed. The highest correlation coefficient was noted for T-score versus maximum failure load (yield stress) of the samples ($r=0.838$, $p<0.001$) as illustrated in Fig. 2.

A similar tendency can be observed for the compressive moduli of the samples, which are calculated based on the linear elastic region of the determined stress–strain curves (Turner and Burr, 1993), as illustrated in Fig. 3.

A limitation however of the introduced process is based on the assumption of the material's isotropy and the determination of universal properties of a bone segment comprising both cortical and cancellous tissue. This methodology was adopted as DXA measurements reflect a combined BMD capturing both bone

Table 1
Descriptive values concerning BMD, T-score and their correlation to the yield stress (σ_y) and elasticity modulus (E).

	BMD (g/cm^2)	T-score	σ_y (MPa)	E (GPa)
Min.	0.4638	−4.47	109.448	12.643
Max.	0.9694	−0.15	218.02	28.536
Mean	0.7248	−2.218	169.996	20.627
S.D.	0.263		24.843	4.129

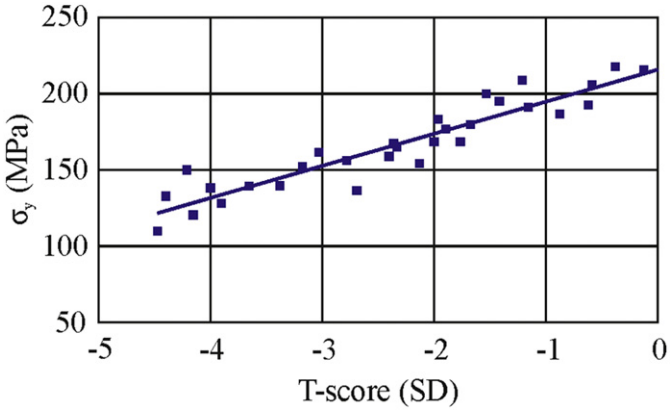

Fig. 2. Equivalent *T*-score values versus yield stress σ_y ($p < 0.001$).

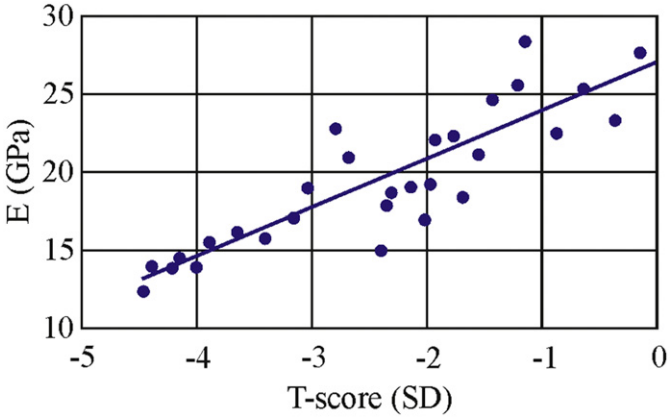

Fig. 3. Equivalent *T*-score values versus elasticity modulus ($p < 0.001$).

types by default and thus the assumption of a compound material is beneficiary to the approach.

4. FEA simulation

In order to associate the ultimate compression strength of the samples to fragility fracture risks of the femoral neck, a model of a human femur was developed, to simulate a gait type loading scenario considering combined multiaxial forces (Jacobs et al., 1997).

Computed Tomography (CT) was employed to reconsider all anatomical aspects in a 3D model. Even though both CT and Magnetic Resonance Imaging (MRI) demonstrate high inherent image contrast between bone and soft tissue, CT is slightly more accurate in the reconstruction of skeletal characteristics, especially when examining longer bones like the femur (Rathnayaka et al., 2012). CT was therefore the imaging technique of choice during this study. This enables relatively unhindered segmentation of bone, allowing the generation of a geometrically accurate volumetric data set of the examined human anatomy. The basic concept is to determine the bone's outline within each CT image and then overlay consecutive slices to reconstruct the examined 3D geometry (Tsouknidas et al., 2011, in press). During the present investigation a patients femur was scanned in its entirety from below its lower boundaries to the upper limit of the femoral head, ensuring the full visual representation of the examined area. Data acquisition was in accordance to Digital Imaging and Communications in Medicine (DICOM) and interpolation of the CT information ensured an isotropic data set. Although this process did not result in higher resolution of the reconstructed set of vertebra, it led to smoother representation allowing the distinct removal of the remaining soft tissue in close proximity to the bone.

The meshing of the volume presented in Fig. 4 was conducted in ANSA of BETA CAE Systems in order to ensure proper element size in all regions and thus a realistic and isotropic stress transition within the considered anatomy. In order to determine the optimum mesh density, convergence studies were conducted. This is achieved through consecutive simulations of a reference load, while altering the mesh density. Once two consecutive simulations result in a 3% deviation of the monitored stress or strain values, the grid is considered as mesh independent and accepted for all further simulations.

During the linear elastic simulation, the specimens were once again considered as a uniform-isotropic material, comprising of a compound bone tissue (reflecting properties of both cortical and cancellous bone), to directly facilitate the correlation of the DXA measurements to the fracture risk of the femoral neck. The experimentally determined mechanical properties were adopted as bulk properties of the compound material and assigned as such in the simulation. The Poisson ratio was assigned as 0.3 corresponding to a mean value of cortical and cancellous bone (Lu et al., 1996; Smit et al., 1997) regardless of DXA value.

The acting loads on the femur comprised a 2317 N joint force (Sarikat and Yildiz, 2011), evenly distributed over the femoral head, inclined by 24° to the coronal plane and 6° to the sagittal one as shown in Fig. 4. The same figure illustrates the abductor muscle force, which was applied to the trochanter and amounted to 703 N, inclined by 28° to the coronal plane and 15° to the sagittal one. The model was bound at a lower section of the femur

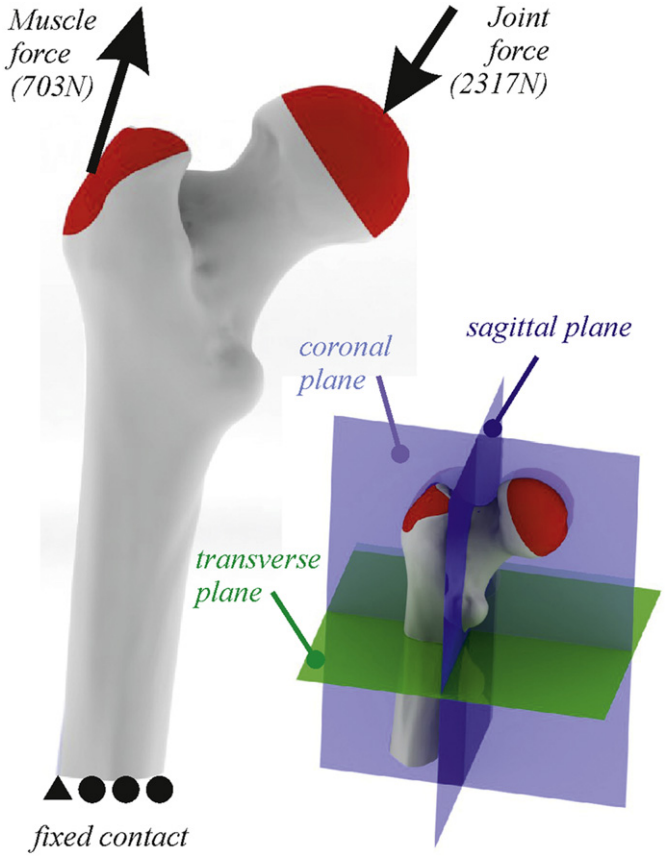

Fig. 4. Applied load and boundary conditions of the developed FEA model.

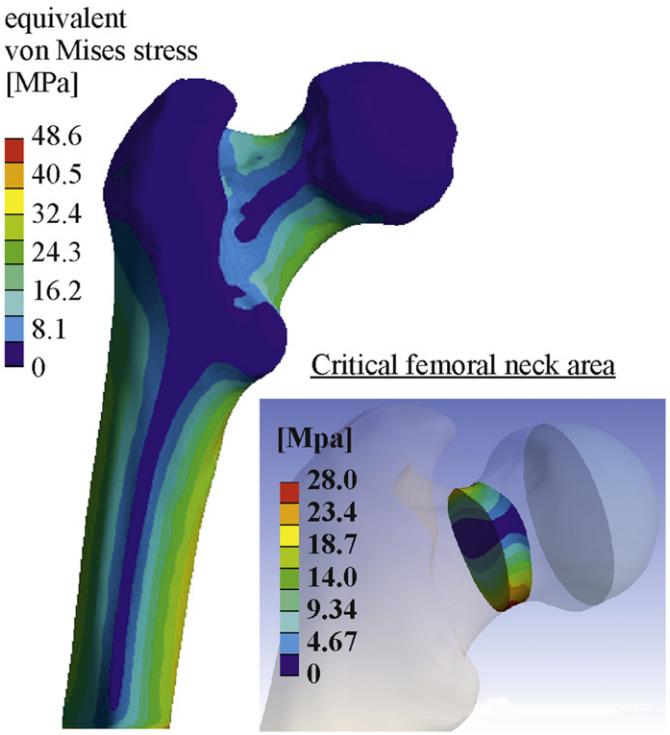

Fig. 5. Calculated stress field on a reverse engineered model of the femur.

to avoid interference of the developing stresses with the reaction of the model's fixation point.

The action of these forces mimics the average loading history encountered during walking of an adult human, corresponding to 10,000 daily cycles as described by Sarikat and Yildiz (2011).

There exists scepticism concerning the ability of compression tests in predicting the hip fracture risk, as fractures in the hip region are the effect of complex dynamic force application, comprising shear, tension and compression. Based on the forgoing description of the model, it becomes evident that the conducted compression experiments capture the loading scenario in a realistic manner, as the compressive strength of the femoral neck exerts a dominant impact on the structural integrity of the femur. Furthermore, the compression tests were identically performed in all cases while the only variations between samples were based on the bone mineral density.

A characteristic stress field developing on the developed model, corresponding to the mean BMD of all conducted experiments (T-score$=-2.218$, $\sigma_y=169.996$ MPa and $E=20.627$ GPa), is demonstrated in Fig. 5.

A closer examination of the critical femoral neck area (shown in the detail of Fig. 5) reveals that the apparent critical stress is concentrated in the superior and inferior regions of the examined samples, sustaining previous findings (deBakker et al., 2009).

5. Discussion

DXA scans in the hip region are conventionally performed in the trochanter, the Ward's triangle and the femoral neck (in an orthogonal area of 6 by 10 mm). The aim of our study was to correlate the BMD obtained from DXA to the mechanical strength characteristics of the examined area, so as to provide surgeons with a DXA based risk assessment concerning fragility fractures.

The introduced experimental investigation affirmed the reliability of BMD in predicting the mechanical properties of the femoral neck. A strong enslavement of the ultimate material strength to BMD ($r=0.838$) was found, while the correlation to elastic modulus ($r=0.689$) was weaker.

There exists a consensus throughout literature, that bone density can be considered as a strong independent predictor of failure strength (Stankewich et al., 1996).

In order to associate the measured BMD of each sample to apparent fracture risk, the developed FEA simulation was considered. Since however, the same geometry, loading and boundary conditions were applied for all simulations and linear elastic properties were considered, the calculated stress field values remain unaffected regardless of the alternation materials elasticity modulus. Therefore another parameter, indicative of the materials response, has to be considered. The equivalent strain is such a characteristic value, unique for each simulation. This approach has a further advantage, as the equivalent strain does not depend on specimen dimensions being a relative value of the apparent deformation (in three directions) to the initial specimen dimensions. This facilitates the consideration of the rather slim specimens used in this study, reflecting the area conventionally considered during DXA measurements, allowing a direct comparison of the attained results.

By overlaying the calculated values with the experimentally determined fracture strain ($\varepsilon=\sigma_y/E$) of the examined specimens, a correlation between T-score and fracture risk can be determined as demonstrated in Fig. 6.

The foregoing FEA simulation however, is based on a static loading case, representing a daily cycle of at least 10,000 loadings. Considering that fracture rarely occurs during walking the maximum calculated strain should account for running, impact or accidental loads, which significantly increase the fracture risk.

It has been reported (Bergmann et al., 1993, 2004) that unexpected loss of balance in a one-legged stance may increase hip contact forces by 52%, whereas stumbling during running results in a 310% augmentation. These factors have been implemented into Fig. 6, designating a shaded area in which the patients BMD poses a major fracture risk during stumbling.

Even though DXA is a cost efficient BMD determinant, dominating the preference of surgeons due to its simplicity, there are some limitations associated to the method that may affect the accuracy of the introduced procedure.

As DXA quantifies the bone mass and not the bone quality of a specific site, micro-fractures in vertical trabeculae of cancellous bone will maintain undetected. It is however widely accepted that micro-fractures exert an important influence on the mechanical strength of the bone. Despite this, DXA can be treated as a macroscopic indicator of bone strength, especially in the hip region, where gait like loading ensures constant remodelling and thus the probability of micro-fractures is considered rather low.

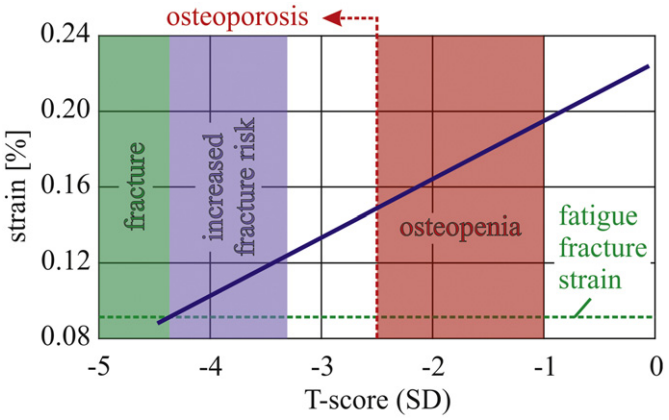

Fig. 6. T-score as a fracture risk indicator.

Another possible limitation of our study is associated to the patients from whom the samples were harvested, as all of them were diagnosed with osteoarthritis. This might have a twofold effect on the BMD–bone properties correlation.

Primary, it has not been established if the most common musculoskeletal disorders of the elderly (osteoarthritis and osteoporosis) may be treated as independent; studies have shown that the presence of one disease may act as a protective against the other (Solomon et al., 1982; Cooper et al., 1991). The effect however of this on the presented results, can be neglected as the selected patients exhibited significant differences in terms of BMD.

Secondary, osteoarthritis has been associated to subchondral scleroses in femoral head; the femoral neck and the trochander region however, are rarely affected by the condition (Li and Aspden, 1997). In order to circumvent this issue, our methodology considered DXA scans in femoral neck, trochanter and Ward's triangle. Additionally, osteoarthritic patients undergoing total hip arthroplasty were the only group of patients from whom we could receive bone samples from the femoral neck region.

Studies have indicated that the femur carries 30% of the applied loads in the subcapital region, while the base of the neck is subjected to 96% of the total load (Lotz et al., 1995). This strengthens the vital role of the femoral neck's capacity to transmit the compressive stress from the joint to the shaft of the femur. Although the aetiology of osteoporotic hip fracture is complex and multifactorial (Melton and Riggs, 1985; Greenspan et al., 1994), bone quality is, without doubt, a major risk factor.

6. Conclusions

Bone mineral density measured by DXA, regardless of limitations associated to the technique's ability to capture bone quality, is a strong predictor of bone strength in the femoral neck region. Supported by an adequate FEA simulation, DXA may be regarded as a valuable tool during the prediction of BMD spectrums which present a significant risk of fragility fractures.

Conflict of interest

The authors would like to state that this work is not subject to any conflict of interest. In these terms, there do not exist any financial or personal relationships with other scientists/people and/or organisations that could have inappropriately influenced our work.

Acknowledgements

The authors would like to thank BETA CAE Systems SA for providing them with the CAE pre-processor ANSA, used during surface and volume generation and meshing of the introduced model.

References

Augat, P., Reeb, H., Claes, L.E., 1996. Prediction of fracture load at different skeletal sites by geometric properties of the cortical shell. Journal of Bone and Mineral Research 11, 1356–1363.

Augat, P., Fan, B., Lane, N.E., Lang, T.F., LeHir, P., Lu, Y., Uffmann, M., Genant, H.K., 1998. Assesment of bone mineral at appendicular sites in females with fractures of the proximal femur. Bone 22, 395–402.

Bergmann, G., Graichen, F., Rohlmann, A., 1993. Hip joint loading during walking and running, measured in two patients. Journal of Biomechanics 26 (8), 969–990.

Bergmann, G., Graichen, F., Rohlmann, A., 2004. Hip joint contact forces during stumbling. Langenbeck's Archives of Surgery 389, 53–59.

Black, D.M., Greenspan, S.L., Ensrud, K.E., Palermo, L., McGowan, J.A., Lang, T.F., Garnero, P., Bouxsein, M.L., Bilezikian, J.P., Rosen, C.J., 2003. The effects of parathyroid hormone and alendronate alone or in combination in postmenopausal osteoporosis. The New England Journal of Medicine 349 (13), 1207–1215.

Bohr, H., Schaadt, O., 1985. Bone mineral content of the femoral neck and shaft: relation between cortical and trabecular bone. Calcified Tissue International 37, 340–344.

Braun, M.J., Meta, M.D., Schneider, P., Reiners, C., 1998. Clinical evaluation of a high-resolution new peripheral quantitative computerized tomography (pQCT) scanner for the bone densitometry at the lower limb. Physics in Medicine and Biology 43, 2279–2294.

Cooper, C., Cook, P.L., Osmond, C., Cawley, M.I.D., 1991. Osteoarthritis of the hip and osteoporosis of the proximal femur. Annals of the Rheumatic Diseases 50, 540–542.

Cooper, C., Campion, G., Melton, L.J., 1992. Hip fractures in the elderly: a world-wide projection. Osteoporosis International 2, 285–289.

Dempster, D.W., 2011. Osteoporosis and the burden of osteoporosis-related fractures. American Journal of Managed Care 17 (6), S164–S169.

Dupree, K., Dobs, A., 2004. Osteopenia and male hypogonadism. Reviews in Urology 6 (6), S30–S34.

deBakker, P., Manske, S., Ebacher, V., Oxland, T., Cripton, P., Guy, P., 2009. During sideways falls proximal femur fractures initiate in the superolateral cortex: evidence from high-speed video of simulated fractures. Journal of Biomechanics 42, 1917–1925.

Ettinger, B., 2008. A personal perspective on fracture risk assessment tools. Menopause: The Journal of The North American Menopause Society 15 (5), 1023–1026.

Frost, H.M., Thomas, C.C., 1963. Bone Remodeling Dynamics. Springfield, IL.

Genant, H.K., Engelke, K., Fuerst, T., Gluer, C.C., Gramp, S., Harris, S.T., et al., 1996. Noninvasive assessment of bone mineral and structure: state of the art. Journal of Bone and Mineral Research 11, 707–730.

Greenspan, S.L., Myers, E.R., Maitland, L.A., Resnick, N.M., Hayes, W.C., 1994. Fall severity and bone mineral density as risk factor for hip fracture in ambulatory elderly. Journal of the American Medical Association 271, 128–133.

Hackett, E.S., MacLeay, J.M., Green, M., Enns, R.M., Pechey, C.L., Les, C.M., Turner, A.S., 2009. Femoral cortical bone mineral density and biomechanical. Properties in sheep consuming an acidifying diet. Nutrition and Metabolic Insights 1, 11–16.

Holick, M.F., 2004. Vitamin D: importance in the prevention of cancers, type 1 diabetes, heart disease, and osteoporosis. American Journal of Clinical Nutrition 79 (3), 362–371.

Jacobs, C.R., Simo, J.C., Beaupre, G.S., Carter, D.R., 1997. Adaptive bone remodeling incorporating simountaneous density and anisotropy considerations. Journal of Biomechanics 30 (6), 603–613.

Keller, T.S., Mao, Z., Spengler, D.M., 1990. Young's modulus, bending strength and tissue physical properties of human compact bone. Journal of Orthopaedic Research 8, 592–603.

Lotz, J.C., Cheal, E.J., Hayes, W.C., 1995. Stress distributions within the proximal femur during gait and falls: implications for osteoporotic fracture. Osteoporosis International 5, 252–261.

Lochmuller, E.M., Miller, P., Burklein, D., Wehr, U., Rambeck, W., Eckstein, F., 2000. In situ femoral DXA related to ash weight, bone size and density and its relationship with mechanical failure loads of the proximal femur. Osteoporosis International 11, 361–367.

Li, B., Aspden, R.M., 1997. Material properties of bone from the femoral neck and calcarfemorale of patients with osteoporosis or osteoarthritis. Osteoporosis International 7, 450–456.

Lu, Y.M., Hutton, W.C., Gharpuray, V.M., 1996. Do bending, twisting and diurnal fluid change in the disc affect the propensity to prolapse? A viscoelastic finite element model. Spine 21, 2570–2579.

Melton, L.J., Riggs, B.L., 1985. Risk factors for injury after a fall. Symposium on falls in the elderly: biological and behavioral aspects. Clinics in Geriatric Medicine 1, 525–39.

Melton 3rd, L.J., Chrischilles, E.A., Cooper, C., Lane, A.W., Riggs, B.L., 1992. Perspective. How many women have osteoporosis? Journal of Bone and Mineral Research 7, 1005–1010.

Minaire, P., 1989. Immobilization osteoporosis: a review. Clinical Rheumatology 8 (2), 95–103.

Newton-John, H.F., Morgan, D.B., 1970. The loss of bone with age, osteoporosis, and fractures. Clinical Orthopaedics and Related Research 71, 229–252.

Old, J.L., Calvert, M., 2004. Vertebral compression fractures in the elderly. American Family Physician 69 (1), 111–116.

Parfitt, A.M., Villanueva, A.R., Foldes, J., Rao, D.S., 1995. Relations between histologic indices of bone formation: implications for the pathogenesis of spinal osteoporosis. Journal of Bone and Mineral Research 10 (3), 466–473.

Reilly, D.T., Burstein, A.H., 1997. The elastic and ultimate properties of compact bone tissue. Journal of Biomechanics 8, 393–405.

Rathnayaka, K., Momot, K.I., Noser, H., Volp, A., Schuetz, M.A., Sahama, T., Schmutz, B., 2012. Quantification of the accuracy of MRI generated 3D models of long bones compared to CT generated 3D models. Medical Engineering & Physics 34 (3), 357–363.

Raisz, L., 2005. Pathogenesis of osteoporosis: concepts, conflicts, and prospects. Journal of Clinical Investigation 115 (12), 3318–3325.

Ray, N.F., Chan, J.K., Thamer, M., Melton, L.J., 1997. Medical expenditures for the treatment of osteoporotic fractures in the United States in 1995: report from

the National Osteoporosis Foundation. Journal of Bone and Mineral Research 12, 24–35.
Rockwood, P.R., Horne, J.G., Cryer., C., 1990. Hip fractures: a future epidemic? Journal of Orthopaedic Trauma 4, 388–396.
Sarikat, M., Yildiz, H., 2011. Determination of bone density distribution in proximal femur by using the 3D orthotropic bone adaption model. Proceedings of the Institute of Mechanical Engineering, Part H: Journal of Engineering in Medicine 225, 365–75.
Stankewich, C.L., Chapman, J., Muthusamy, R., 1996. Relationship of mechanical factors to the strength of proximal femur fractures fixed with cancellous screws. Journal of Orthopaedic Trauma 10, 248–257.
Solomon, L., Schnitzler, C.M., Browett, J.P., 1982. Osteoarthritis of the hip: the patient behind the disease. Annals of the Rheumatic Diseases 41, 118–125.
Smit, T.H., Odgaard, A., Schneider, E., 1997. Structure and function of vertebral trabecular bone. Spine 22, 2823–2833.
St-Onge, M.P., Wang, J., Shen, W., Wang, Z., Allison, D.B., Heshka, S., Pierson, R.N., Heymsfield, S.B., 2004. Dual-energy X-ray absorptiometry-measured lean soft tissue mass: differing relation to body cell mass across the adult life span. Journals of Gerontology Series A: Biological Sciences and Medical Sciences 59 (8), 796–800.
Tsouknidas, A., Maropoulos, S., Savvakis, S., Michailidis, N., 2011. FEM assisted evaluation of PMMA and Ti_6Al_4V as materials for cranioplasty resulting mechanical behaviour and the neurocranial protection. Bio-Medical Materials and Engineering 21 (3), 139–147.
Turner, C.H., Burr, D.B., 1993. Basic biomechanical measurements of bone: a tutorial. Bone 14, 595–608.
Tsouknidas, A., Michailidis, N., Savvakis, S., Anagnostidis, A., Bouzakis, K.D., Kapetanos, G. A FEM modelling technique to determine the mechanical response of a lumbar spine segment under complex loads. Journal of Applied Biomechanics, in press.
World Health Organisation, 1994. Assessment of Fracture Risk and Its Application to Screening for Postmenopausal Osteoporosis. WHO, Geneva Technical Report Series.